β2-adrenoreceptor Signaling Increases Therapy Resistance in Prostate Cancer by Upregulating MCL1

Sazzad Hassan[1,2], Ashok Pullikuth[1], Kyle C. Nelson[1], Anabel Flores[1], Yelena Karpova[1], Daniele Baiz[1], Sinan Zhu[1], Guangchao Sui[1], Yue Huang[1], Young A. Choi[1], Ralph D'Agostino Jr[3], Ashok Hemal[4], Urs von Holzen[2,5], Waldemar Debinski[1,3,6], and George Kulik[1,3,4,7]

ABSTRACT

There is accumulating evidence that continuous activation of the sympathetic nervous system due to psychosocial stress increases resistance to therapy and accelerates tumor growth via β2-adrenoreceptor signaling (ADRB2). However, the effector mechanisms appear to be specific to tumor type. Here we show that activation of ADRB2 by epinephrine, increased in response to immobilization stress, delays the loss of MCL1 apoptosis regulator (MCL1) protein expression induced by cytotoxic drugs in prostate cancer cells; and thus, increases resistance of prostate cancer xenografts to cytotoxic therapies. The effect of epinephrine on MCL1 protein depended on protein kinase A (PKA) activity, but was independent from androgen receptor expression. Furthermore, elevated blood epinephrine levels correlated positively with an increased MCL1 protein expression in human prostate biopsies. In summary, we demonstrate that stress triggers an androgen-independent antiapoptotic signaling via the ADRB2/PKA/MCL1 pathway in prostate cancer cells.

Implications: Presented results justify clinical studies of ADRB2 blockers as therapeutics and of MCL1 protein expression as potential biomarker predicting efficacy of apoptosis-targeting drugs in prostate cancer.

Introduction

Prostate cancer is routinely treated with androgen ablation therapy with initial success but with subsequent development of androgen-independent prostate cancer (1). These tumors are often more aggressive, have increased metastatic capacity, and are refractory to further treatment. Therefore, identifying the mechanism(s) of therapy resistance is of extreme importance (1, 2).

The diagnosis of cancer and its treatment can often lead to psychologic stress and depression in patients (3, 4). Physiologic and psychologic stress has been linked with tumor progression and aggressiveness (5–10). Both acute and chronic forms of stress change endocrine status, including increased serum levels of epinephrine. Recent work has demonstrated that physiologically relevant levels of epinephrine protect prostate cancer cells in tissue culture and *in vivo* from apoptosis when treated with chemotherapeutics or androgen ablation (11, 12), providing a link between stress and therapeutic resistance. The analysis of the underlying mechanisms identified ADRB2/PKA/BCL2-associated agonist of cell death (BAD) as a sig-

naling pathway connecting increased epinephrine levels with apoptosis inhibition. However, epinephrine may use other mechanisms beside BAD phosphorylation to inhibit apoptosis.

MCL1, an antiapoptotic protein with short half-life, has been connected with antiapoptotic signaling in several cancers including prostate cancer (13, 14). Because of the central role of MCL1 in apoptosis and the potential for PKA to regulate MCL1 protein levels (15), we hypothesized that epinephrine signaling protects prostate cancer cells from apoptosis by increasing MCL1 protein level. In this work, we demonstrate that epinephrine when added to culture medium at physiologically relevant concentrations, delays loss of MCL1 in prostate cancer cells treated with inhibitors of PI3K and of protein synthesis or with clinically used chemotherapeutics estramustine and mitoxantrone, resulting in protection of apoptosis. Effects of epinephrine depended on PKA activity, but were independent from the expression of androgen receptors (AR). Furthermore, injection of epinephrine or subjecting mice to stress preserved MCL1 expression and increased resistance of prostate cancer xenografts to cytotoxic therapies with combination of PI3K inhibitor and prostate-targeted toxin J591-PE. Finally, blood epinephrine levels and MCL1 expression were positively correlated in human prostate biopsies. Taken together, our results identify the epinephrine/ADRB2/PKA/MCL1 pathway as new mechanism that may contribute to therapeutic resistance in advanced androgen-independent prostate cancer.

Materials and Methods

Human study participants and sample collection

Selection of the study participants and collections of blood and prostate biopsy samples were conducted in accordance with recognized ethical guidelines (e.g., Declaration of Helsinki, CIOMS, Belmont Report, U.S. Common Rule) and followed the protocol approved by the Wake Forest University Health Sciences Institutional Review Board as described previously (16). Written informed consent was obtained from all patients who provided samples for the study.

[1]Department of Cancer Biology, Wake Forest School of Medicine, Winston-Salem, North Carolina. [2]Indiana University School of Medicine-South Bend, South Bend, Indiana. [3]Comprehensive Cancer Center, Wake Forest School of Medicine, Winston-Salem, North Carolina. [4]Department of Urology, Wake Forest School of Medicine, Winston-Salem, North Carolina. [5]Goshen Center for Cancer Care, Goshen, Indiana. [6]Brain Tumor Center of Excellence, Wake Forest School of Medicine, Winston-Salem, North Carolina. [7]Department of Life Sciences, Alfaisal University, Riyadh, Kingdom of Saudi Arabia.

Note: Supplementary data for this article are available at Molecular Cancer Research Online (http://mcr.aacrjournals.org/).

Corresponding Author: George Kulik, Wake Forest School of Medicine, Medical Center Blvd., Winston-Salem, NC 27157. Phone: 336-713-7650; Fax: 336-713-7650; E-mail: gkulik@wakehealth.edu

Epinephrine measurements

Plasma epinephrine concentrations were measured by ELISA, using commercially available assays (BA-0100 from Labor Diagnostika) purchased through Rocky Mountain Diagnostics as described previously (12).

Plasmids and transfection

FLAG-MCL1 construct and short hairpin RNA (shRNA) constructs driven by the U6 promoter that target MCL1 coding and 3′UTR sequences (5-AATTCAAAAAATTGTTTAACTCGCCAGTCCCG-TA-3 and 5-GTAGCCAGGCAAGTCATAGAATA-3 respectively) were described previously (13). The single shRNA targeting the AR (5-TGCTGAAGAGTAGCAGTGCTTTTTTC-3) used was described previously (11). A scrambled RNA oligonucleotide sequence (GGTACGGTCAGGCAGCTTCT) was used as a control. Cell cultures grown to 60%–70% confluency were transfected using Lipofectamine 2000 (Invitrogen) according to the manufacturer's recommendations, or infected with lentivirus generated by HEK293 cells as described previously (17).

Doxycycline-inducible MCL1 shRNA system

Inducible MCL1 shRNA lentiviral vectors were constructed as described previously (18). Briefly, two oligonucleotides (i) MCL1-shRNA-S: 5′-AGCGGTAGCCAGGCAAGTCATAGAAT<u>TAGTGA-AGCCACAGATGTA</u>ATTCTATGACTTGCCTGGCTAA-3′ and (ii) MCL1-shRNA-AS: 5′-GGCATTAGCCAGGCAAGTCATAGAAT-TACATCTGTGGCTT<u>CACTA</u>ATTCTATGACTTGCCTGGCTAC-3′ were annealed to create BfuA1 overhangs and ligated to BfuA1 digested pEN-TGmiRc entry vector. Sequence-confirmed clones were used to transfer shRNA template into the pSLIK-Zeo vector through site-specific LR clonase reaction (Gateway, Invitrogen). This platform uses miR-30a architecture with 5′, 3′ UTR and stem loop (underlined, above) derived from miR30a sequence. Similarly, nontargeting scrambled vector was generated by annealing the following oligonucleotides (MCL1-DY-scr-S: 5′-AGCGGGTACGGTCAGGCAGCTTCTAT-T<u>AGTGAAGCCACAGATGTA</u>ATAGAAGCTGCCTGACCGTA-CA-3′ and MCL1-DY-scr-AS: 5′-GGCATGTACGGTCAGGC-AGCTTCTATT<u>ACATCTGTGGCTTCACTA</u>ATAGAAGCTGC-CTGACCGTACC-3′) and subsequent site-specific recombination into the pSLIK-Zeo vector as described above (18). Lentiviral particles were generated by cotransfection of HEK293T cells with pSLIK-Zeo-shRNA expression vectors and third-generation lentivirus packaging and VSV-G pseudotyping plasmids (19) at the Cell Engineering Core facility, Wake Forest University Comprehensive Cancer Center (WFUCCC, Winston-Salem, NC).

Cell lines, antibodies, and reagents

C4-2LucPKI, C4-2Luc, PC3, and LNCaP cell lines used in this study were described previously (12, 13). To generate stable cell line expressing inducible MCL1-shRNA and scrambled shRNA, C4-2Luc cells were transduced with inducible shRNA lentiviral particles and stable clones were selected with addition of Zeocin (500 μg/mL). MCL1 knockdown was initiated with the addition of doxycline (2 μg/mL). Induction of shRNA is coupled with GFP expression under the TET-inducible (TRE) system enabling visual confirmation of GFP expression and MCL1 knockdown confirmed by Western blot analysis. Cell lines were tested for *Mycoplasma* at Cell Engineering Shared Resource laboratory WFUCCC (Winston-Salem, NC).

Antibodies were obtained from the following sources: mouse mAb to β-actin from Sigma-Aldrich; rabbit polyclonal antibody to MCL1 from Stressgene; β-actin from Sigma; rabbit polyclonal antibodies to AR from Cell Signaling Technology, secondary horseradish peroxidase–conjugated antibodies from Amersham Biosciences. Anti-Rabbit IgG IRDye800 Goat Polyclonal Conjugated Secondary Antibody and anti-Mouse IgG IRDye680LT Goat Polyclonal Conjugated Secondary Antibody (used for Odyssey Western blots) were obtained from LI-COR Biosciences. ZSTK474 from Zenyaku-Kogyo Co. Ltd. G418 was from Clontech. J591PE was produced as described earlier (20). ICI118,551 was a gift from Dr. Raymond Penn (Thomas Jefferson University, Philadelphia, PA). Tissue culture reagents were purchased from Invitrogen. Thapsigargin, LY294002, forskolin, doxycycline, H7, and all other chemicals and reagents, unless otherwise specified, were purchased from Sigma-Aldrich.

Western blot analysis

Analysis of prostate biopsy samples and cell lysates by Western blotting was described previously (16) The Odyssey CLx Infrared Imaging System (LI-COR Biosciences) was used according to the manufacturer's instructions for imaging of Western blots. Protein bands were quantified using Odyssey imaging software, ImageJ software (NIH, Bethesda, MD), or Adobe Photoshop.

Mean gray value (MGV) for MCL1 was measured by Image J and corrected for β-actin MGV by following formula: (raw MGV_MCL1)* (lowest MGV_β-actin)/(raw MGV_β-actin).

Xenograft model

All animal studies complied with the NIH Guide for the Care and Use of Laboratory Animals and were approved by the Institutional Animal Care and Use Committee of Wake Forest School of Medicine and of University of Notre Dame (Notre Dame, IN).

Six-week-old male Balb/c-nu/nu were obtained from Charles River. Mice were maintained under pathogen-free conditions and provided with sterile food and water *ad libitum*. Human tumor xenografts were generated by subcutaneously inoculating prostate cancer cell lines (C4-2Luc) into nude mice. Each mouse received four subcutaneous injections of 2×10^6 cells with BD Matrigel matrix High Concentration (BD Biosciences). Injections were made using an insulin syringe and a 27-gauge needle at four locations: left and right shoulder and left and right flank. Injections at four locations ensured that each mouse would develop xenograft tumors, thus reducing the number of mice required for the experiments. When the largest tumor was approximately 100 mm³ in size, mice were randomly assigned to experimental groups: DMSO (30 μL); ZSTK474 (375 μg/kg) +J591PE (2.5 mg/kg); ZSTK474 + J591PE followed 3 hours later by immobilization stress; ZSTK474 + J591PE followed 3 hours later by epinephrine (100 μmol/L, 30 μL). DMSO, ZSTK474, and J591PE were delivered by intratumoral injections. In experiments where doxycycline-induced constructs were used, mice were injected with doxycycline (intraperitoneal, 1 mg/g of body weight) and provided with drinking water supplemented with 1 mg/mL of doxycycline 24 hours prior to injections of cytotoxic drugs.

Immobilization stress, which mimicked the presence of a natural predator without possibility of escape, was created by placing mice into a 50-mL conical vial with openings for breathing. Vials with mice were placed for 1 hour in a plastic box that contained tissue impregnated with fox urine (Chagnon Trapping Supply). Details of stress procedure, imaging of tumor luminescence and extraction of proteins from xenograft tumors have been described previously (12).

Analysis of apoptosis

Time-lapse microscopy: Cells were plated in 6-well plates and transfected by Lipofectamine with a GFP-tagged MCL1-specific shRNA or scrambled shRNA (control); or mixture of constructs of

FLAG-MCL1 and EGFP (3:1). After 48 hours, cells were serum starved overnight (16 hours) before treatments with the combination of LY294002 and thapsigargin; epinephrine, or DMSO as a control. GFP$^+$ cells were followed by time-lapse video recording that was analyzed for the percentage of cells with apoptotic morphology (assessed as cytoplasmic blebbing and fragmentation). For these experiments, at least four randomly chosen fields (containing on average 100–200 cells for each treatment) were recorded. Details of this procedure were described previously (21). The results reported herein were confirmed by at least three independent experiments.

Statistical analysis

Statistical analyses were performed using SAS and Excel software.

For analyses that included repeated measures for luminescence, a repeated measures mixed model was fit with the mouse considered as a random effect in the model and treatment group (ZSTK474 + J591PE, ZSTK474 + J591PE+stress, ZSTK474 + J591PE+epinephrine, or Control) and time (0, 24, 48 or 72 hours) considered as fixed effects. The treatment group-by-time interaction was examined first in these models; if nonsignificant, then that term was removed. If the overall time-by-group interaction was significant, we examined pairs of groups over a time period (i.e., ZSTK474 + J591PE+stress vs. ZSTK474 + J591PE+stress, etc.). Comparisons were made using these mixed models.

We found significant time-by-group interactions for the ZSTK474 + J591PE vs. ZSTK474 + J591PE+epinephrine model and the ZSTK474 + J591PE vs. ZSTK474 + J591PE+stress model ($P = 0.02$ and 0.04, respectively). There was no significant time-by-group interaction for the ZSTK474 + J591PE+epinephrine versus ZSTK474 + J591PE+stress comparison ($P = 0.72$), suggesting that rate of luminescence change across time differed for the ZSTK474 + J591PE+epinephirne or ZSTK474 + J591PE+stress groups when compared with ZSTK474 + J591PE alone—but not when compared with each other.

Statistical analysis of percent apoptosis was done by two-tailed t test.

Results

Epinephrine inhibits apoptosis by upregulation of MCL1 in prostate cancer cells

In LNCaP and C4-2 prostate cancer cell lines treatment with the PI3K inhibitor induced apoptosis within 18–24 hours. However, simultaneously inhibiting a protein synthesis (with cycloheximide or thapsigargin) and a PI3K (by ZSTK474 or LY294002) resulted in MCL1 loss which coincided with increased apoptosis within 6 hours (13). Thapsigargin, that triggers endoplasmic reticulum (ER) stress has been routinely used by our group in combination with PI3K inhibitors to induce rapid apoptosis in prostate cancer cells (11, 17, 21). Thapsigargin-based chemotherapeutic mipsagargin is currently in clinical trials for treatment-refractory metastatic cancers (22). Epinephrine can protect prostate cancer cells from apoptosis when treated with a cytotoxic combination of thapsigargin and LY294002 (11). In C4-2 prostate cancer cells treated with epinephrine, loss of MCL1 protein was delayed by 6 hours (**Fig. 1A**). Dose-response analysis showed that effects on MCL1 began at 1 nmol/L of epinephrine (**Fig. 1B**), which is comparable with blood concentrations of epinephrine during chronic stress (23).

To examine the generality of epinephrine-induced increase of MCL1 level, we tested the effects of proapoptotic treatments, with or without epinephrine, on MCL1 levels in other prostate cancer cells.

Just as in C4-2 cells, when human prostate cancer cell lines PC3 and LNCaP were treated with LY294002 and thapsigargin, MCL1 expression was decreased. Consistent with the results of experiments in C4-2 cells, MCL1 loss was delayed by treatment with10 nmol/L epinephrine in both PC3 and LNCaP cells (Supplementary Fig. S1A and S1B). We also tested the effects of estramustine and mitoxantrone used for chemotherapy in advanced prostate cancer. Similarly to combinations of PI3K inhibitor and thapsigargin, estramustine and mitoxantrone decreased expression of MCL1 in prostate cancer cells, whereas treatments with Epi restored MCL1 expression (Supplementary Figs. S4 and S5A).
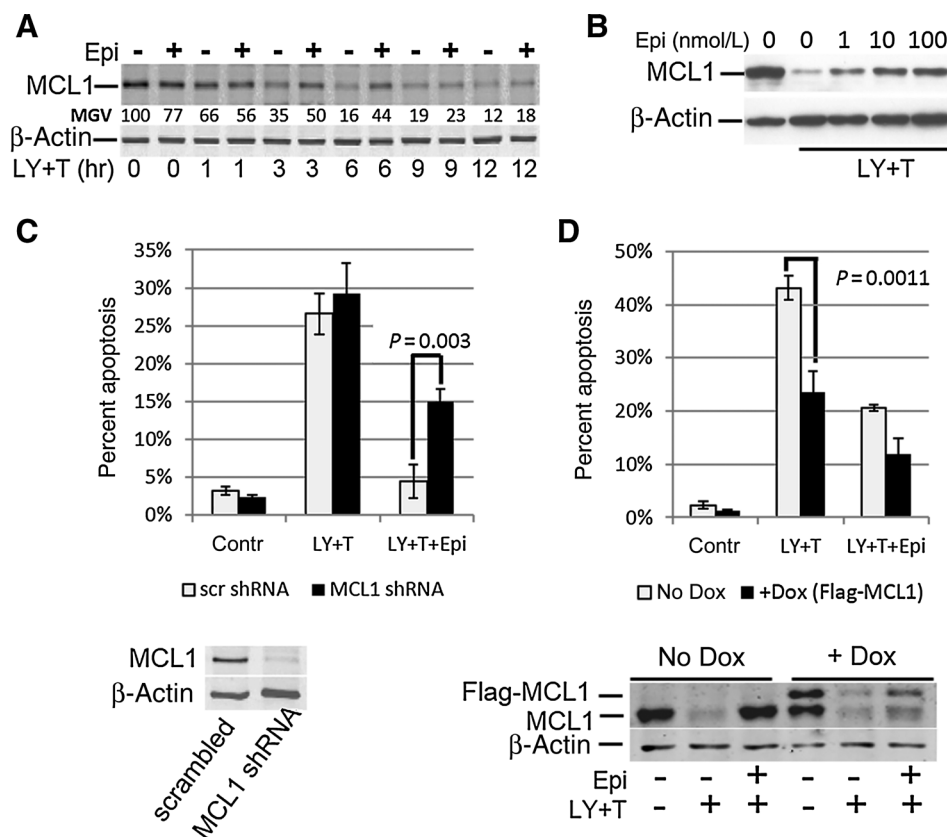
To examine the role of MCL1 in the antiapoptotic effects of epinephrine, we used the previously characterized MCL1 shRNA construct that coexpresses EGFP (13) to knock down MCL1 expression (**Fig. 1C**). Time-lapse microscopy was used to track fluorescently labeled C4-2 cells after transfection with either shRNA-targeting MCL1 or scrambled shRNA. We then compared apoptosis rates between C4-2 cells treated with cytotoxic combination plus epinephrine and cells transfected with either scrambled shRNA or MCL1 shRNA. MCL1 knockdown diminished the antiapoptotic effects of epinephrine when C4-2 cells were subjected to cytotoxic treatment (**Fig. 1C**; Supplementary Fig. S1C).

To further confirm MCL1 as a mediator of epinephrine's antiapoptotic effects, we used a FLAG-tagged MCL1 (FLAG-MCL1) expression construct under the control of a doxycycline-inducible promoter to overexpress FLAG-MCL1. When C4-2 cells were transfected with this inducible MCL1 expression construct and incubated with doxycycline, FLAG-MCL1 was detectable by Western blot analysis (**Fig. 1D**). In cells treated with cytotoxic combination, FLAG-MCL1 expression and endogenous MCL1 had comparable decreases. Just as with endogenous MCL1, decrease of FLAG-MCL1 expression was prevented when cells were treated with cytotoxic combination plus epinephrine (**Fig. 1D**). When FLAG-MCL1 was ectopically expressed in C4-2 cells, the rate of apoptosis at 6 hours was decreased from 43% to 24%, which is comparable with apoptosis in cells treated with cytotoxic combination and epinephrine (**Fig. 1D**; Supplementary Fig. S1D). This delay of apoptosis occurred despite the decrease of FLAG-MCL1 levels, perhaps because total MCL1 in doxycycline-treated cells was still elevated after treatment with cytotoxic combination (MGV for endogenous MCL1 without doxycycline is 12.3; MGV for endogenous MCL1 and FLAG-MCL1 with doxycycline is 20.2; in lanes 2 and 5, respectively, in **Fig. 1D** inset, see Supplementary Fig. S1E for quantitation).

Collectively, these experiments demonstrate that increased MCL1 levels contribute to the antiapoptotic effects of epinephrine, and establish MCL1 as a functional target of epinephrine's antiapoptotic signaling.

Epinephrine regulates MCL1 via the ADRB2/PKA pathway

The ADRB2 are the major receptors for epinephrine in human prostates and prostate cancer cells (24, 25). To examine the role of ADRB2 in regulation of MCL1 protein levels, C4-2 cells were treated with cytotoxic combination plus 10 nmol/L epinephrine and 100 nmol/L of the ADRB2-selective antagonist ICI118,551 (26). Epinephrine-induced increase of MCL1 levels was abrogated in the presence of ICI118,551 (**Fig. 2A**, lanes 3 vs. 6), implicating ADRB2 in this phenomenon. Similar effects of ICI118,551 on Epi regulation of MCL1 were observed in LNCaP and PC3 cells (Supplementary Fig. S2A) and in C4-2 cells treated with chemotherapeutic agents Estramustine or Mitoxantrone (Supplementary Fig. S5B).
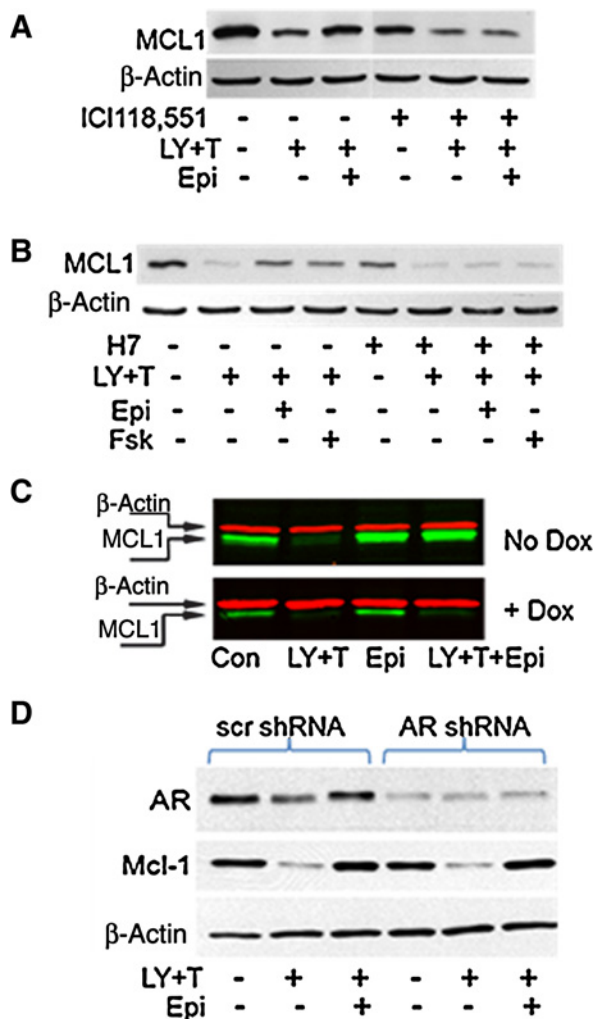
Figure 1.
Epinephrine inhibits apoptosis by upregulating MCL1 in prostate cancer cells. **A,** Time course of MCL1 downregulation. C4-2 cells were treated with combination of 25 μmol/L LY294002 and 1 μmol/L thapsigargin (LY+T) either with or without 10 nmol/L epinephrine (Epi) and lysed after indicated time. Cell lysates were analyzed by Western blotting with antibodies against MCL1 and β-actin (loading control). Intensities of MCL1 signals (MGV) were measured using Image J software as described in "Materials and Methods." **B,** Dose response of epinephrine's effects. C4-2 cells were treated with LY+T and indicated concentrations of Epi. Lysates where collected within 6 hours and analyzed as in **A**. **C,** MCL1 is required for antiapoptotic effect of epinephrine. C4-2 cells were infected with lentiviral vectors that express either scrambled or MCL1 shRNA, treated with combinations of LY+T and Epi as indicated and cell death was followed by time-lapse video recording. Bar graphs show percent apoptosis 6 hours after treatments Apoptosis in epinephrine-treated cells with MCL1 knockdown was significantly higher comparing with cells that express scrambled shRNA (*P* = 0.003). Inset panel below shows MCL1 knockdown. **D,** Increased expression of MCL1 inhibits cell death induced by LY+T combination. C4-2 cells were transfected with pTRE-tight vector that express Flag-MCL1 under doxycylin (Dox)-sensitive promoter. Forty-eight hours later, cells were treated with doxycycline followed by treatments with LY+T and Epi. Cell death was followed by time-lapse video recording. Bar graphs show apoptosis 6 hours after treatments. Apoptosis in cells that overexpressed MCL1 is significantly reduced (*P* = 0.0011). Two-tailed homoscedastic *t* test was used for the statistical analysis. Inset panel below shows Flag-MCL1 expression in cells treated with doxycyclin. Extended time-lapse data for C and D are shown in Supplementary Fig. S1C and S1D. MGV of MCL1 shown in Supplementary Fig. S1E.

In prostate epithelial cells ADRB2 is coupled to Gα$_s$βγ complex, which upon ligand binding triggers activation of adenylyl cyclase followed by activation of PKA. To investigate the role of the signaling pathways downstream of ADRB2 in epinephrine-dependent increase of MCL1 protein levels, we treated C4-2 cells with forskolin. Forskolin directly activates adenylyl cyclase, resulting in production of cyclic adenosine monophosphate (cAMP). In the presence of cytotoxic combination and 5 μmol/L forskolin, MCL1 expression was retained (**Fig. 2B**, lane 2 vs. lane 4). Thus, activation of adenylyl cyclase is sufficient to increase MCL1 in response to epinephrine treatment. Because PKA is a well-established mediator of ADRB2/cAMP signaling, we utilized the PKA inhibitors H7 and PKI (27) to test the role of PKA in regulation of MCL1 protein levels. H7 prevented MCL1 regulation by either 10 nmol/L epinephrine or 5 μmol/L forskolin in C4-2 cells when treated with cytotoxic combination (**Fig. 2B**; compare lanes 3 and 7). Similar effects on MCL1 levels were observed in LNCaP

and PC3 cells (Supplementary Fig. S2B) and in C4-2 cells treated with chemotherapeutic agents estramustine or mitoxantrone (Supplementary Fig. S5C and S5D).

To confirm the role of PKA in epinephrine-induced regulation of MCL1, we stably transfected a previously described doxycycline-inducible construct that expresses the PKA peptide inhibitor PKI-GFP chimera into C4-2Luc cells (12, 28). These C4-2Luc-PKI cells were then incubated with cytotoxic combination and 10 nmol/L epinephrine. PKA inhibition by PKI prevented epinephrine from restoring MCL1 protein levels (**Fig. 2C**; compare lane 4 doxycycline vs. no doxycycline panels). Thus, blocking ADRB2 signaling by an inverse ADRB2 agonist ICI118,551 or a PKA inhibitor effectively abrogates regulation of MCL1 levels by epinephrine. At the same time, artificially activating PKA with forskolin mimics the effects of epinephrine on MCL1 protein expression. Taken together, these results establish the role of the

Figure 2.
Epinephrine upregulates MCL1 via the ADRB2/PKA pathway. **A,** Effects of epinephrine on MCL1 are mediated via ADRB2. C4-2 cells were treated with combination of LY+T, Epi (as in **Fig. 1**) and 100 nmol/L ICI118,551 (selective antagonist of ADRB2) as indicated. Expression of MCL1 was analyzed by Western blotting in cell lysates prepared 6 hours after treatments. **B,** Effects of epinephrine are blocked by a pharmacologic PKA inhibitor. C4-2 cells were treated with combination of LY+T, Epi, 5 μmol/L forskolin (Fsk), and 100 μmol/L PKA inhibitor H7 as indicated. Cells were lysed 6 hours after treatments and expression levels of MCL1 were analyzed by Western blotting. **C,** Effects of epinephrine are blocked by the PKA inhibitor peptide PKI. C4-2PKI cells that inducibly express the PKIGFP peptide inhibitor of PKA were treated with the combination of LY+T, Epi, or doxycycline as indicated. Expression of MCL1 was detected by Western blotting. To control for equal protein loading, lysates were probed for β-actin. **D,** Epinephrine-induced upregulation of MCL1 is AR independent. Cells were infected with lentiviral vectors that expressed either scrambled or AR-targeting shRNAs and treated with the combination of LY+T and epinephrine. Expression of MCL1 was detected by Western blotting. To control for equal loading, lysates were probed for β-actin.

ADRB2/cAMP/PKA signaling pathway in regulation of MCL1 by epinephrine.

Previous studies in prostate cancer cells have demonstrated that the PKA pathway can activate the AR in an androgen-independent manner (29). To examine the possible role of AR in the epinephrine-dependent stabilization of MCL1, we introduced a shRNA targeting the AR into C4-2 prostate cancer cells. As shown in **Fig. 2D**, AR knockdown did not prevent regulation of MCL1 by epinephrine. These results demonstrate that activated PKA regulates MCL1 without involving AR.

Concentrations of epinephrine found during stress restore MCL1 expression in cells treated with J591PE

Chimeras of *Pseudomonas aeruginosa exotoxin* (PE, which functions as a translational inhibitor) fused to tumor-specific antibodies or growth factors have been proposed as targeted therapy for cancers (30). By fusing PE to the anti-PSMA antibody J591 (J591PE), PE can be selectively delivered to prostate cells that express PSMA (20). Treating C4-2Luc cells with the combination of J591PE chimeric antibody and ZSTK474 induced apoptosis and involution of prostate cancer xenografts (20).
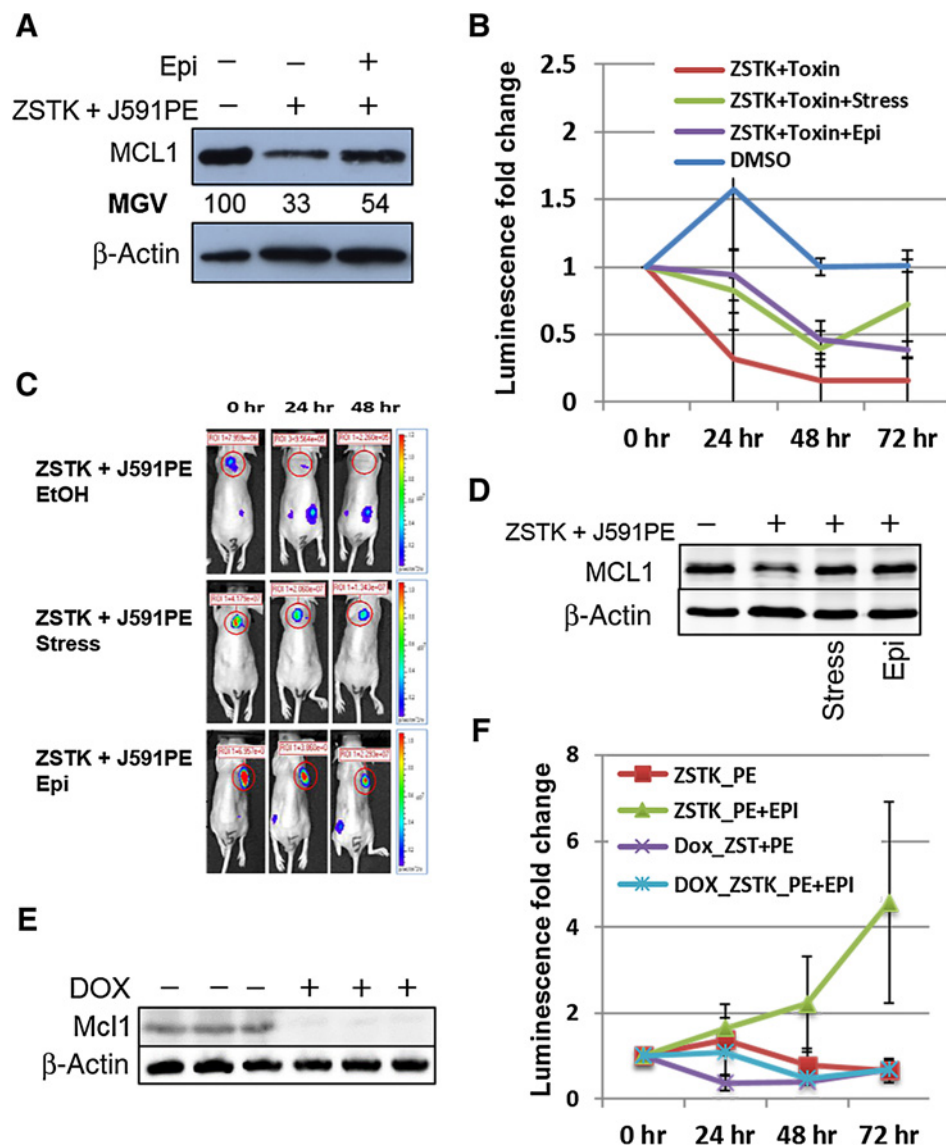
When C4-2Luc prostate cancer cells were treated with 1 μg/mL of J591PE in combination with 5 μmol/L of the PI3K inhibitor ZSTK474, MCL1 expression decreased, whereas epinephrine diminished the MCL1 loss (**Fig. 3A**).

In humans, serum epinephrine levels increase above baseline from 0.05–0.1 nmol/L up to 1–15 nmol/L in response to psychoemotional or physical stress (31). Likewise, in mouse models, blood serum levels of epinephrine increase up to 1–15 nmol/L in response to immobilization stress (12). To test whether stress will interfere with targeted therapies, we examined luminescence in C4-2Luc xenografts treated with J591PE and ZSTK474 in calm and stressed mice and in mice injected with epinephrine.

Previously, we used MRI and IHC to demonstrate that luminescence of C4-2Luc xenografts adequately reflects tumor burden, and that decreased luminescence in xenografts treated by PI3K inhibitors was accompanied by increased apoptosis (12). The combination of J591PE and ZSTK474 rapidly decreased tumor burden, as measured by luminescence, over a 48-hour period (**Fig. 3B** and **C**; Supplementary Fig. S3A). However, when cytotoxic combination treatment was followed by either immobilization stress or injection of epinephrine (100 μmol/L, 30 μL), decrease in bioluminescence was significantly less comparing with xenografts that receive cytotoxic treatments only ($P = 0.04$ and $P = 0.02$, respectively; **Fig. 3B** and **C**). No significant differences were detected between tumor luminescence in stressed mice and in mice injected with epinephrine ($P = 0.72$), which is consistent with our earlier reports that adrenergic signaling is primarily responsible for tumor-promoting effects of stress (12).

To examine the effects of stress and epinephrine injections on MCL1 levels *in vivo*, xenograft tumors were excised 6 hours after mice were injected with cytotoxic agents followed by stress or epinephrine injection. In agreement with tissue culture studies, cytotoxic agents decreased MCL1 levels in C4-2Luc xenografts, whereas subjecting mice to immobilization stress or injections with epinephrine prevented the decrease of MCL1 (**Fig. 3D**).

To test the role of MCL1 in tumor-promoting effects of epinephrine, we generated C42shMCL1 cells that constitutively express firefly luciferase and inducibly express MCL1-specific shRNA upon treatment with doxycycline (Supplementary Fig. S3B and S3C). C42shMCL1 cells produced luminescent xenograft tumors. Providing doxycycline to these mice induced loss of MCL1 expression in C42shMCL1 xenografts (**Fig. 3E**). Analysis of the effects of epinephrine on the luminescence of C42shMCL1 xenograft tumors injected with ZSTK474 and J591PE showed that similarly to C4-2luc xenografts, injections of epinephrine significantly increased luminescence in C42shMCL1 xenografts in mice that did not receive doxycycline. In contrast, no significant differences in luminescence with and without

Hassan et al.

Figure 3.
Stress-induced concentrations of epinephrine preserve MCL1 expression in prostate cancer xenografts treated with J591PE. **A,** Epinephrine prevents MCL1 loss in C4-2Luc cells treated with the combination of J591PE toxin and the PI3K inhibitor ZSTK474. C4-2Luc cells were treated with the combination of J591PE, ZSTK474, or Epi as indicated. After 6 hours, lysates were prepared and analyzed for MCL1 and for β-actin (loading control) by Western blotting. Intensities of MCL1 signals (MGV, mean gray values) were measured using Image J software as described in "Materials and Methods." **B,** Stress and epinephrine inhibit involution of C4-2Luc prostate cancer xenografts induced by combination of ZSTK474 and J591PE. Graph shows fold change in luminescence of C4-2Luc xenografts in mice injected with DMSO (blue line, $n = 3$), ZSTK474 and J591PE (red line, $n = 3$), ZSTK474 and J591PE followed by immobilization stress (green line, $n = 3$) or by injection of epinephrine (purple line, $n = 5$). Statistical analyses by t test showed significantly increased tumor luminescence in mice subjected to stress or injected with epinephrine compared with mice that received only ZSTK474 and J591PE ($P = 0.04$ and $P = 0.02$, respectively). Data for individual tumors are shown in Supplementary Fig. S3A. **C,** Representative images of mice with luminescent C4-2Luc xenografts. **D,** Immobilization stress and epinephrine prevent MCL1 loss in C4-2Luc xenograft tumors. Xenografts were excised from mice treated as in **B** 6 hours after treatments. Expression levels of MCL1 analyzed as in **A**. **E,** Knockdown of MCL1 in C4-2shMCL1 xenografts induced by doxycycline (Dox). Xenografts were excised 24 hours after mice were either injected intraperitoneally with doxycycline (1 g/kg) or left untreated and MCL1 expression was analyzed by Western botting. **F,** Inducible knockdown of MCL1 prevents Epi-induced protection from cytotoxic therapies. Graph shows fold change in luminescence of C42shMCL1 xenografts in mice injected with ZSTK474 and J591PE (red squares, $n = 10$), and in mice injected with ZSTK474 and J591PE followed by injection of epinephrine (green triangles, $n = 5$). Statistical analyses by t test showed significantly increased tumor luminescence in mice without doxycycline injected with Epi (green and red lines; $P = 0.03$; $n = 10, 5$). In contrast, no significant differences in luminescence between tumors injected with ZSTK474 and J591PE (blue stars, $n = 3$) and in mice injected with ZSTK474 and J591PE followed by injection of epinephrine (purple crosses, $n = 3$), was observed in mice that receive doxycycline and had MCL1 knockdown in C42shMCL1 xenografts (blue and purple lines; $P = 0.97$; $n = 3, 3$). Data for individual tumors are shown in Supplementary Fig. S3D.

epinephrine injections were observed in C42shMCL1 xenografts in which MCL1 expression knocked down was induced by providing mice with doxycycline (**Fig. 3F**; Supplementary Fig. S3D).

Taken together, data from xenograft experiments confirm that increased epinephrine levels in response to stress could regulate MCL1 protein in prostate tumors *in vivo*; and that increase of MCL1 protein expression contributes to cytoprotective and tumor-promoting effects of epinephrine.

Elevated serum epinephrine levels correlate with increased MCL1 in prostate biopsies

Because epinephrine protects prostate cancer cells in culture from apoptosis and prevents loss of MCL1 expression in tissue culture and in prostate cancer xenografts, we examined possible associations between blood levels of epinephrine and MCL1 protein expression in human prostate tissue. To do so, we compared MCL1 protein levels in prostate biopsies from patients with high and low levels of epinephrine in their blood (**Fig. 4A**). In agreement with the results from tissue culture and xenograft models, increased MCL1 expression in prostate biopsies was positively correlated with increased blood epinephrine levels. When we analyzed all samples, the Spearman correlation was $\rho = 0.69$ ($P = 0.009$); after removal of patient 14, an outlier with extremely high epinephrine levels, the Pearson correlation was $\rho = 0.74$ ($P = 0.005$) and the Spearman correlation was $\rho = 0.73$ ($P = 0.007$; **Fig. 4B**). These results suggest that MCL1 expression is regulated by the epinephrine/ADRB2/PKA pathway, and that MCL1 expression contributes to the antiapoptotic and tumor-promoting effects of psychoemotional stress in men.

Discussion

Our results demonstrate that epinephrine can render prostate cancer cells resistant to apoptosis via upregulation of MCL1, a highly labile antiapoptotic protein of the BCL2 family. Furthermore, this study establishes that upregulation of MCL1 protein is mediated by the ADRB2/PKA pathway in a cAMP-dependent manner. Our animal studies show that epinephrine or behavioral stress can increase MCL1 protein expression and decrease efficacy of targeted therapies in prostate cancer xenografts.
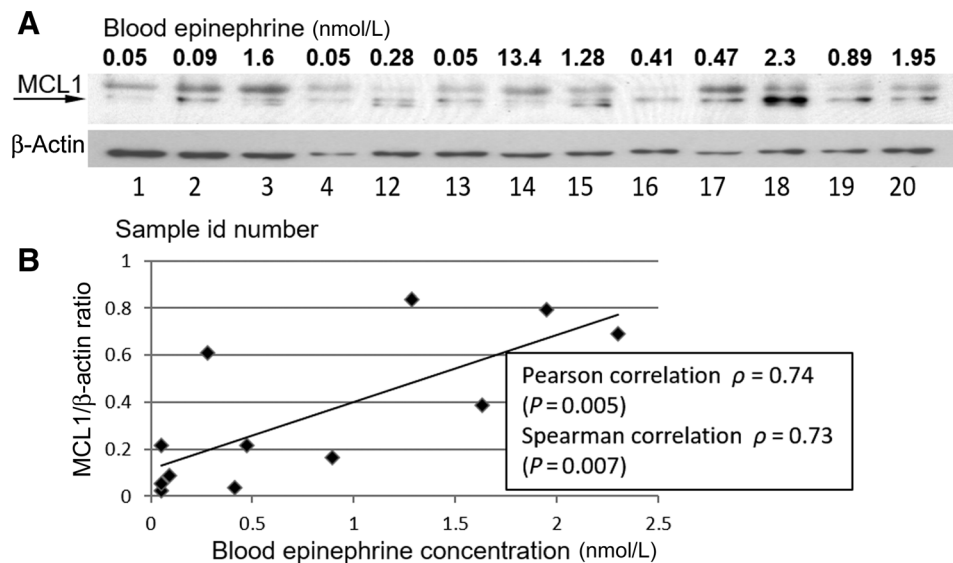
Epidemiologic studies have been equivocal regarding the connection between prostate cancer and stress (32–35). While it remains controversial as to whether emotional stress increases cancer incidence, several reports agree that emotional stress can influence cancer progression (36, 37). The evidence is accumulating that catecholamines released systemically from adrenal glands or locally from sympathetic nerves act on cancer cells and the tumor microenvironment to inhibit apoptosis, accelerate vascularization, migration, and invasion in several tumor models including prostate cancer (12, 36, 38–44). Earlier data established a biochemical link between emotional stress and chemotherapeutic resistance. Thus, physiologically relevant levels of epinephrine can confer apoptotic resistance to chemotherapeutics in prostate cancer cells and experimental prostate tumors, via activation of the ADRB2/PKA/BAD pathway (11). These experiments demonstrated that PI3K inhibitors plus protein synthesis inhibitors can cause the proapoptotic BH3 only protein BAD to be dephosphorylated at Ser112 in prostate cancer cells, resulting in cell death. In addition, when prostate cancer cells were exposed to epinephrine, even in the presence of PI3K inhibitors and protein synthesis inhibitors, BAD became phosphorylated and thus deactivated, resulting in protection from apoptosis (11). In these earlier experiments, however, the expression of a phosphodeficient BAD did not block antiapoptotic effects of epinephrine completely, suggesting that BAD is not the only target of epinephrine signaling.

A role of MCL1 in apoptosis regulation in prostate cancer cells and a synergism between loss of MCL1 and BAD dephosphorylation is supported by recent experimental work (13). By overexpressing a phosphodeficient BAD protein in combination with knockdown of MCL1 by shRNA, the apoptotic rate in prostate cancer cells was comparable with apoptosis in prostate cancer cells treated with a PI3K inhibitor and a protein synthesis inhibitor (13).

MCL1 localizes to the outer mitochondrial membrane, where it acts as an antiapoptotic protein by inhibiting BAX and BAK oligomerization and to the mitochondrial matrix where it regulates energy production (45). MCL1 protein is characterized by a short half-life that is dynamically regulated by posttranslational modification (45, 46). MCL1 is larger than other members of the BCL2 family due to an extended amino terminal end region that contains multiple PEST

Figure 4.

MCL1 expression in prostate biopsies. **A,** Proteins extracted from prostate biopsies analyzed by Western blotting for MCL1 and β-actin. Arrow points at the MCL1 band. Numbers under the blot indicate the patient identification number; numbers above the blot show blood levels of epinephrine. **B,** Relative intensity of MCL1 band (MCL1/β-actin) plotted against epinephrine concentrations in blood collected before biopsies. Pearson and Spearman correlations shown in the box were calculated after removing data for the outlier (patient #14).

(Proline, Glutamic acid, Serine and Threonine) domains. The PEST domains are targets of a complex posttranslational modification scheme which regulates MCL1 activity and stability (47). MCL1 is differentially phosphorylated by multiple kinases that affect MCL1 half-life through regulating its proteosomal degradation (47). Extracellular signals that trigger different phosphorylation states of MCL1 result in either an increase or a decrease in protein half-life (47, 48). MCL1 is also regulated transcriptionally by the transcription factor cAMP response element binding protein (CREB) in some cancers. When CREB is activated by phosphorylation, it can bind to a cAMP response element located within the endogenous *MCL1* promoter, resulting in transcriptional activation (49).

MCL1 is upregulated in many cancers, including prostate, providing them a mechanism to escape apoptosis and confer resistance to antitumor therapies (50–53), at the same time chemotherapeutics used in advanced prostate cancer can decrease MCL1 expression (Supplementary Fig. S4). However, the mechanisms of MCL1 regulation in prostate cancer are unclear.

Because the AR pathway plays a central role in prostate physiology, we examined its contribution to regulation of MCL1 levels, and demonstrated that epinephrine restores MCL1 expression independently from AR.

To further elucidate the signaling mechanism of epinephrine, we examined the role of PKA, a known mediator of ADRB2 signaling (54, 55), in regulation of MCL1 levels. By selectively either inhibiting or activating PKA, we demonstrated that MCL1 protein level is dependent on PKA activity (**Fig. 2B**; Supplementary Fig. S5C and S5D). In the presented experiments, we used protein synthesis inhibitors, therefore regulation of MCL1 protein levels by PKA most likely occurs at posttranscriptional level. At the same time, transcription factor CREB is a target of PKA activity, and *MCL1* transcription is regulated by CREB, providing a possible mechanism for transcriptional regulation of MCL1 (49, 56). The exact mechanisms of MCL1 regulation by PKA in prostate tumors require further investigation.

In this work, we demonstrated that epinephrine signaling via the ADRB2/PKA pathway increased levels of the antiapoptotic protein MCL1 in prostate cancer cells. Similar to results in tissue culture models, increased levels of MCL1 were observed in xenografts in mice subjected to immobilization stress or injected with epinephrine. Finally, blood epinephrine levels and expression of MCL1 were positively correlated in prostate biopsies. In summary, our findings argue that epinephrine signaling can contribute to the pathophysiology of advanced androgen-independent prostate cancer, and that ADRB2 should be evaluated as a therapeutic target in patients with advanced prostate cancer.

Experiments presented here, together with earlier publications, bring to light a robust antiapoptotic signaling network in prostate cancer that links the PI3K and the ADRB2/PKA pathways with the proteins of the BCL2 superfamily BAD and MCL1 (**Fig. 5**; ref. 57). In clinical trials, PI3K inhibitors did not show clear benefits for patients with prostate cancer (58–61), which may be due to the activation of other antiapoptotic pathways that compensate for the loss of PI3K activity. Together with earlier publications from our group and others, results presented here further justify clinical testing of inhibiting ADRB2 in prostate cancer. Because ADRB2 blockers are already approved for clinical use, the challenge is to identify patients who would benefit from repurposing β-blockers as anticancer therapeutics. Our results suggest that monitoring downstream effectors of the apoptosis regulatory network—BAD phosphorylation and MCL1 expression—may predict whether targeted therapies that aim at
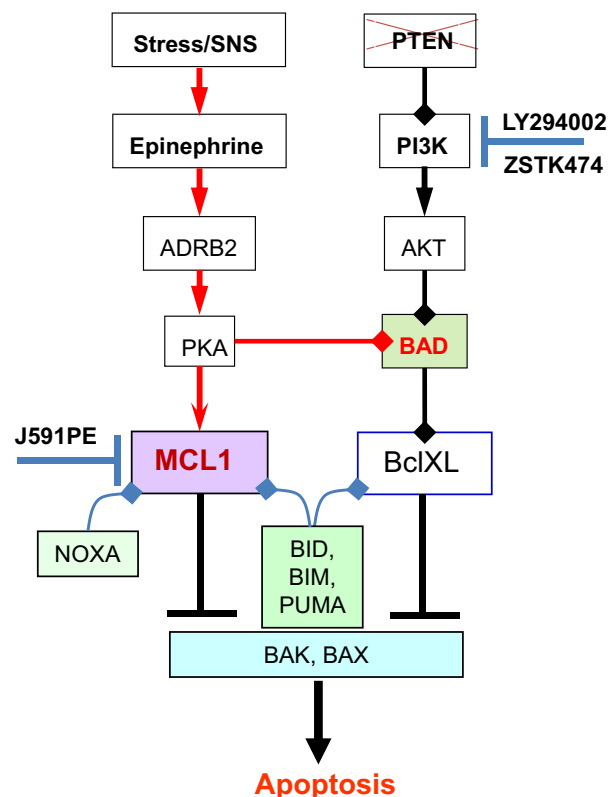

Figure 5.
Epinephrine prevents degradation of MCL1 and inactivates BAD. Dual targeting of the apoptosis regulatory network at MCL1 and BAD explains potent antiapoptotic effect of epinephrine in prostate cancer.

inhibiting PI3K, ADRB2 or other pathways that regulate apoptosis would help patients with prostate cancer.

Disclosure of Potential Conflicts of Interest

Authors' Contributions

S. Hassan: Conceptualization, resources, investigation. **A. Pullikuth:** Resources, investigation. **K.C. Nelson:** Investigation. **A. Flores:** Investigation. **Y. Karpova:** Investigation. **D. Baiz:** Investigation. **S. Zhu:** Investigation. **G. Sui:** Investigation. **Y. Huang:** Investigation. **R. D'Agostino:** Formal analysis. **A. Hemal:** Resources. **U. von Holzen:** Supervision, writing-review and editing. **W. Debinski:** Resources, supervision. **G. Kulik:** Conceptualization, supervision, funding acquisition, validation, investigation, writing-original draft, project administration, writing-review and editing.

Acknowledgments

References

1. Shen MM, Abate-Shen C. Molecular genetics of prostate cancer: new prospects for old challenges. Genes Dev 2010;24:1967–2000.
2. Burgess EF, Roth BJ. Changing perspectives of the role of chemotherapy in advanced prostate cancer. Urol Clin North Am 2006;33:227–36.
3. Spiegel D, Giese-Davis J. Depression and cancer: mechanisms and disease progression. Biol Psychiatry 2003;54:269–82.
4. Sklar LS, Anisman H. Stress and cancer. Psychol Bull 1981;89:369–406.
5. Armaiz-Pena GN, Lutgendorf SK, Cole SW, Sood AK. Neuroendocrine modulation of cancer progression. Brain Behav Immun 2009;23:10–5.
6. Campbell JP, Karolak MR, Ma Y, Perrien DS, Masood-Campbell SK, Penner NL, et al. Stimulation of host bone marrow stromal cells by sympathetic nerves promotes breast cancer bone metastasis in mice. PLoS Biol 2012;10:e1001363.
7. Hassan S, Karpova Y, Flores A, D'Agostino R Jr, Kulik G. Surgical stress delays prostate involution in mice. PLoS One 2013;8:e78175.
8. Neeman E, Ben-Eliyahu S. Surgery and stress promote cancer metastasis: new outlooks on perioperative mediating mechanisms and immune involvement. Brain Behav Immun 2013;30:S32–40.
9. Schuller HM, Al-Wadei HA. Beta-adrenergic signaling in the development and progression of pulmonary and pancreatic adenocarcinoma. Curr Cancer Ther Rev 2012;8:116–27.
10. Eng JW, Reed CB, Kokolus KM, Pitoniak R, Utley A, Bucsek MJ, et al. Housing temperature-induced stress drives therapeutic resistance in murine tumour models through β2-adrenergic receptor activation. Nat Commun 2015;6:6426.
11. Sastry KS, Karpova Y, Prokopovich S, Smith AJ, Essau B, Gersappe A, et al. Epinephrine protects cancer cells from apoptosis via activation of cAMP-dependent protein kinase and BAD phosphorylation. J Biol Chem 2007;282: 14094–100.
12. Hassan S, Karpova Y, Baiz D, Yancey D, Pullikuth A, Flores A, et al. Behavioral stress accelerates prostate cancer development in mice. J Clin Invest 2013;123: 874–86.
13. Yancey D, Nelson KC, Baiz D, Hassan S, Flores A, Pullikuth A, et al. BAD dephosphorylation and decreased expression of MCL-1 induce rapid apoptosis in prostate cancer cells. PLoS One 2013;8:e74561.
14. Cavarretta IT, Neuwirt H, Untergasser G, Moser PL, Zaki MH, Steiner H, et al. The antiapoptotic effect of IL-6 autocrine loop in a cellular model of advanced prostate cancer is mediated by Mcl-1. Oncogene 2007;26: 2822–32.
15. Ozaki Y, Kato T, Kitagawa M, Fujita H, Kitagawa S. Calpain inhibition delays neutrophil apoptosis via cyclic AMP-independent activation of protein kinase A and protein kinase A-mediated stabilization of Mcl-1 and X-linked inhibitor of apoptosis (XIAP). Arch Biochem Biophys 2008;477:227–31.
16. Hassan S, Karpova Y, Flores A, D'Agostino R Jr, Danhauer SC, Hemal A, et al. A pilot study of blood epinephrine levels and CREB phosphorylation in men undergoing prostate biopsies. Int Urol Nephrol 2014;46:505–10.
17. Sastry KS, Karpova Y, Kulik G. Epidermal growth factor protects prostate cancer cells from apoptosis by inducing BAD phosphorylation via redundant signaling pathways. J Biol Chem 2006;281:27367–77.
18. Shin KJ, Wall EA, Zavzavadjian JR, Santat LA, Liu J, Hwang JI, et al. A single lentiviral vector platform for microRNA-based conditional RNA interference and coordinated transgene expression. Proc Natl Acad Sci U S A 2006;103: 13759–64.
19. Dull T, Zufferey R, Kelly M, Mandel RJ, Nguyen M, Trono D, et al. A third-generation lentivirus vector with a conditional packaging system. J Virol 1998;72: 8463–71.
20. Baiz D, Hassan S, Choi YA, Flores A, Karpova Y, Yancey D, et al. Combination of the PI3K inhibitor ZSTK474 with a PSMA-targeted immunotoxin accelerates apoptosis and regression of prostate cancer. Neoplasia 2013;15:1172–83.
21. Sastry KS, Smith AJ, Karpova Y, Datta SR, Kulik G. Diverse antiapoptotic signaling pathways activated by vasoactive intestinal polypeptide, epidermal growth factor, and phosphatidylinositol 3-kinase in prostate cancer cells converge on BAD. J Biol Chem 2006;281:20891–901.
22. Mahalingam D, Wilding G, Denmeade S, Sarantopoulas J, Cosgrove D, Cetnar J, et al. Mipsagargin, a novel thapsigargin-based PSMA-activated prodrug: results of a first-in-man phase I clinical trial in patients with refractory, advanced or metastatic solid tumours. Br J Cancer 2016;114:986–94.
23. Gold SM, Zakowski SG, Valdimarsdottir HB, Bovbjerg DH. Higher Beck depression scores predict delayed epinephrine recovery after acute psychological stress independent of baseline levels of stress and mood. Biol Psychol 2004;67: 261–73.
24. Nagmani R, Pasco DS, Salas RD, Feller DR. Evaluation of beta-adrenergic receptor subtypes in the human prostate cancer cell line-LNCaP. Biochem Pharmacol 2003;65:1489–94.
25. Goepel M, Wittmann A, Rübben H, Michel MC. Comparison of adrenoceptor subtype expression in porcine and human bladder and prostate. Urol Res 1997; 25:199–206.
26. O'Donnell SR, Wanstall JC. Evidence that ICI 118, 551 is a potent, highly beta 2-selective adrenoceptor antagonist and can be used to characterize beta-adrenoceptor populations in tissues. Life Sci 1980;27:671–7.
27. Cheng HC, van Patten SM, Smith AJ, Walsh DA. An active twenty-amino-acid-residue peptide derived from the inhibitor protein of the cyclic AMP-dependent protein kinase. Biochem J 1985;231:655–61.
28. Guo M, Pascual RM, Wang S, Fontana MF, Valancius CA, Panettieri RA Jr, et al. Cytokines regulate beta-2-adrenergic receptor responsiveness in airway smooth muscle via multiple PKA- and EP2 receptor-dependent mechanisms. Biochemistry 2005;44:13771–82.
29. Sarwar M, Sandberg S, Abrahamsson PA, Persson JL. Protein kinase A (PKA) pathway is functionally linked to androgen receptor (AR) in the progression of prostate cancer. Urol Oncol 2014;32:25.e1–12.
30. Debinski W, Karlsson B, Lindholm L, Siegall CB, Willingham MC, FitzGerald D, et al. Monoclonal antibody C242-Pseudomonas exotoxin A. A specific and potent immunotoxin with antitumor activity on a human colon cancer xenograft in nude mice. J Clin Invest 1992;90:405–11.
31. Wortsman J, Frank S, Cryer PE. Adrenomedullary response to maximal stress in humans. Am J Med 1984;77:779–84.
32. Perron L, Bairati I, Harel F, Meyer F. Antihypertensive drug use and the risk of prostate cancer (Canada). Cancer Causes Control 2004;15:535–41.
33. Rodriguez C, Jacobs EJ, Deka A, Patel AV, Bain EB, Thun MJ, et al. Use of blood-pressure-lowering medication and risk of prostate cancer in the Cancer Prevention Study II Nutrition Cohort. Cancer Causes Control 2009;20:671–9.
34. Grytli HH, Fagerland MW, Fossa SD, Tasken KA, Haheim LL. Use of β-blockers is associated with prostate cancer-specific survival in prostate cancer patients on androgen deprivation therapy. Prostate 2013;73:250–60.

35. Shah SM, Carey IM, Owen CG, Harris T, Dewilde S, Cook DG. Does β-adrenoceptor blocker therapy improve cancer survival? Findings from a population-based retrospective cohort study. Br J Clin Pharmacol 2011;72: 157–61.

36. Armaiz-Pena GN, Allen JK, Cruz A, Stone RL, Nick AM, Lin YG, et al. Src activation by β-adrenoreceptors is a key switch for tumour metastasis. Nat Commun 2013;4:1403.

37. Grytli HH, Fagerland MW, Fossa SD, Tasken KA. Association between use of β-blockers and prostate cancer-specific survival: a cohort study of 3561 prostate cancer patients with high-risk or metastatic disease. Eur Urol 2014; 65:635–41.

38. Sood AK, Armaiz-Pena GN, Halder J, Nick AM, Stone RL, Hu W, et al. Adrenergic modulation of focal adhesion kinase protects human ovarian cancer cells from anoikis. J Clin Invest 2010;120:1515–23.

39. Cole SW, Nagaraja AS, Lutgendorf SK, Green PA, Sood AK. Sympathetic nervous system regulation of the tumour microenvironment. Nat Rev Cancer 2015;15:563–72.

40. Thaker PH, Han LY, Kamat AA, Arevalo JM, Takahashi R, Lu C, et al. Chronic stress promotes tumor growth and angiogenesis in a mouse model of ovarian carcinoma. Nat Med 2006;12:939–44.

41. Le CP, Nowell CJ, Kim-Fuchs C, Botteri E, Hiller JG, Ismail H, et al. Chronic stress in mice remodels lymph vasculature to promote tumour cell dissemination. Nat Commun 2016;7:10634.

42. Palm D, Lang K, Niggemann B, Drell TL, Masur K, Zaenker KS, et al. The norepinephrine-driven metastasis development of PC-3 human prostate cancer cells in BALB/c nude mice is inhibited by beta-blockers. Int J Cancer 2006;118: 2744–9.

43. Hulsurkar M, Li Z, Zhang Y, Li X, Zheng D, Li W. Beta-adrenergic signaling promotes tumor angiogenesis and prostate cancer progression through HDAC2-mediated suppression of thrombospondin-1. Oncogene 2017;36: 1525–36.

44. Zahalka AH, Arnal-Estape A, Maryanovich M, Nakahara F, Cruz CD, Finley LWS, et al. Adrenergic nerves activate an angio-metabolic switch in prostate cancer. Science 2017;358:321–6.

45. Perciavalle RM, Opferman JT. Delving deeper: MCL-1's contributions to normal and cancer biology. Trends Cell Biol 2013;23:22–9.

46. Morel C, Carlson SM, White FM, Davis RJ. Mcl-1 integrates the opposing actions of signaling pathways that mediate survival and apoptosis. Mol Cell Biol 2009;29: 3845–52.

47. Thomas LW, Lam C, Edwards SW. Mcl-1; the molecular regulation of protein function. FEBS Lett 2010;584:2981–9.

48. Zhong Q, Gao W, Du F, Wang X. Mule/ARF-BP1, a BH3-only E3 ubiquitin ligase, catalyzes the polyubiquitination of Mcl-1 and regulates apoptosis. Cell 2005;121:1085–95.

49. Wang JM, Chao JR, Chen W, Kuo ML, Yen JJ, Yang-Yen HF. The antiapoptotic gene mcl-1 is up-regulated by the phosphatidylinositol 3-kinase/Akt signaling pathway through a transcription factor complex containing CREB. Mol Cell Biol 1999;19:6195–206.

50. Krajewska M, Krajewski S, Epstein JI, Shabaik A, Sauvageot J, Song K, et al. Immunohistochemical analysis of BCL2, bax, bcl-X, and mcl-1 expression in prostate cancers. Am J Pathol 1996;148:1567–76.

51. Trivigno D, Essmann F, Huber SM, Rudner J. Deubiquitinase USP9x confers radioresistance through stabilization of Mcl-1. Neoplasia 2012;14:893–904.

52. Nijhawan D, Fang M, Traer E, Zhong Q, Gao W, Du F, et al. Elimination of Mcl-1 is required for the initiation of apoptosis following ultraviolet irradiation. Genes Dev 2003;17:1475–86.

53. Wertz IE, Kusam S, Lam C, Okamoto T, Sandoval W, Anderson DJ, et al. Sensitivity to antitubulin chemotherapeutics is regulated by MCL1 and FBW7. Nature 2011;471:110–4.

54. Pierce KL, Premont RT, Lefkowitz RJ. Seven-transmembrane receptors. Nat Rev Mol Cell Biol 2002;3:639–50.

55. Cox ME, Deeble PD, Bissonette EA, Parsons SJ. Activated 3′,5′-cyclic AMP-dependent protein kinase is sufficient to induce neuroendocrine-like differentiation of the LNCaP prostate tumor cell line. J Biol Chem 2000;275:13812–8.

56. Shaywitz AJ, Greenberg ME. CREB: a stimulus-induced transcription factor activated by a diverse array of extracellular signals. Annu Rev Biochem 1999;68: 821–61.

57. Kulik G. ADRB2-targeting therapies for prostate cancer. Cancers 2019;11:358.

58. Bendell JC, Rodon J, Burris HA, de Jonge M, Verweij J, Birle D, et al. Phase I, dose-escalation study of BKM120, an oral pan-Class I PI3K inhibitor, in patients with advanced solid tumors. J Clin Oncol 2012;30:282–90.

59. Zenyaku Kogyo Co., Ltd. A phase 1b, multi-center, open label, uncontrolled, serial cohort, dose escalation study of the safety, tolerability, pharmacokinetics and preliminary efficacy of daily oral doses of ZSTK474 in subjects with advanced solid malignancies. Boston, MA: Dana-Farber Cancer Institute; 2012. Available from: http://clinicaltrials gov/ct2/show/NCT012804872012.

60. U.S. National Library of Medicine. Duke University. BKM120 in metastatic castration-resistant prostate cancer. Novartis Pharmaceuticals; 2012. Available from: http://clinicaltrials gov/ct2/show/NCT01385293.

61. U.S. National Library of Medicine. Sarah Cannon Research Institute. Study of PI3 kinase/mTOR inhibitor BEZ235 twice daily for advanced solid tumors. Novartis; 2012. Available from: http://clinicaltrials gov/ct2/show/NCT01343498.

Molecular Cancer Research

β2-adrenoreceptor Signaling Increases Therapy Resistance in Prostate Cancer by Upregulating MCL1

Sazzad Hassan, Ashok Pullikuth, Kyle C. Nelson, et al.

Updated version	Access the most recent version of this article at: doi:10.1158/1541-7786.MCR-19-1037

E-mail alerts	Sign up to receive free email-alerts related to this article or journal.
Reprints and Subscriptions	To order reprints of this article or to subscribe to the journal, contact the AACR Publications Department at pubs@aacr.org.
Permissions	To request permission to re-use all or part of this article, use this link http://mcr.aacrjournals.org/content/early/2020/10/28/1541-7786.MCR-19-1037. Click on "Request Permissions" which will take you to the Copyright Clearance Center's (CCC) Rightslink site.